IV-4 OPERATING DYNAMICS AND PERFORMANCE LIMITATIONS OF FERRITE DIGITAL PHASE SHIFTERS

G.P. Rodrigue, J.L. Allen, L.J. Lavedan and D.R. Taft

Sperry Microwave Electronics Company

Concerted efforts expended in the development of waveguide ferrite digital phase shifters have resulted in significant contributions to a precise understanding of these devices. The technology has now progressed to a point where rather definite performance capabilities and limitations can be discussed. Achievable phase shift and loss are normally restricted by constraints imposed by the intended application. Optimum performance clearly must be defined in the light of size, weight, and power handling ability requirements.

Digital computers may be used to distinct advantage in optimizing ferrite device designs. While computer-aided analytical approaches are not quite a practical cure all, they can significantly shorten and simplify the usual cut and try experimental approach. The successful utilization of computer-aided analyses requires the application of an accurate mathematical model of the physical structure involved and the development of a suitable technique for obtaining numerical solution of the pertinent boundary value problems.

The results of a computer-aided solution[1] of the ferrite loaded waveguide problem have been corroborated by experimental results and used to accurately predict performance of practical devices as a function of geometry and material parameters. Such techniques enable the engineer to run through a large number of trial geometries in a matter of minutes and readily study the many possible compromises free of the confusing, non-reproducible variables that so often plague microwave device development. While analytical solutions[2, 3] of phase shifter problems have been frequently used as a guide to device design, the ability to precisely predict device performance in terms of intrinsic material parameters permits a level of design accuracy not previously attainable.

Figure 1 is an example of the ability of such solutions to predict both differential phase shift and insertion loss per 360° (LP 360) of differential phase shift. The basic waveguide geometry studied is a single dielectric-loaded toroid as indicated. The results indicate that the optimization of such structure can be accurately carried out by analytical means and that, through proper dielectric loading, both phase shift per unit loss and phase shift per unit length can be maximized.

In this analysis, the magnetic loss in the material is accounted for by the "intrinsic" linewidth of the material. This linewidth is that expected on the given material in the absence of inhomogeneous broadening mechanisms that scatter to degenerate spinwaves. Since, in the normal condition of digital phase shifter operation, there are no long or intermediate wavelength spinwaves degenerate with the operating frequency and, since inhomogeneities are usually too coarse to scatter significantly to very short wavelength spinwaves, it is reasonable to assume that such inhomogeneous broadening mechanisms will not then contribute significantly to magnetic loss. The value of intrinsic linewidth can be obtained from single crystal data on material of equal quality and/or from parallel pump measurements of ΔH_k. In the latter case, the frequency dependence of ΔH_k must be considered in determining the intrinsic linewidth, since the spinwaves of a parallel pump measurement are oscillating at one half the operating frequency. Figure 2 shows the excellent agreement obtained between theoretically predicted and measured loss values, not only for a series of garnets with values of intrinsic linewidth controlled by rare earth doping (points 1 through 6), but also for a magnesium manganese ferrite (point 7).

Figure 3, showing loss per 360° differential phase shift as a function of saturation magnetization, again illustrates the accuracy of the analytical approach. The differential phase shift decreases in proportion to m_r, but losses arising from dielectric loss and waveguide losses remain fixed. Thus at low value of normalized saturation magnetization $\left(m_s = \frac{\gamma 4\pi M_s}{\omega}\right)$, loss increases roughly as $1/m_s$. At large values of m_s the loss again increases sharply, this time due to the encroachment of resonance loss. The width of the flat, low loss region is quite dependent on the values of intrinsic linewidth and anisotropy field.

As a result of these considerations, one is lead to consider as an "optimum" design, i.e. one producing maximum phase shift per unit loss, a device employing an m_s value of 0.6 to 0.8 with a minimum intrinsic linewidth and a resonable degree of dielectric loading of the toroid slot. Such designs result in figures of merit of the order of 1000 degrees/db.

In practice, operational requirements will impose restrictions that cause modifications in this "optimum" design. As an example, high peak or average power handling requirements usually require a change in the device geometry or material selection. High peak power requirements can be met by either material or geometric adjustments. The peak power handling ability of a material can be increased by increasing the ΔH_k (and hence intrinsic linewidth) or by decreasing the saturation magnetization of the material. Figure 4 shows the critical field values (and corresponding power levels in the geometry of Figure 1) as a function of m_s with ΔH_k as a parameter. Some increase in loss must be expected in return for this increase in peak power capability as can be deduced from the results shown in Figures 2 and 3. At this time, however, it appears that for a device with a maximum insertion loss of 1 db per 360°, peak power levels in excess of 150 KW at X-band, 400 KW at C-band, and 750 KW at S-band should be manageable.

The handling of high average rf power levels usually requires some change in the component design. The principal difficulty is in dissipating the heat generated by losses in the ferrite. The effectiveness of cooling the waveguide is limited because the poor heat conductivity of ferrite results in the center portion of the ferrite toroid being essentially insulated from the waveguide walls by the rest of the toroid. Several techniques are available to minimize the effects of the temperature dependence of $4\pi M_s$ such as flux drive, composite toroids, temperature compensated garnets and programming of the electronic driver. Any technique whic reduces the loss/length in the ferrite will also help by reducing the absorbed power In addition, the use of various thermal conducting dielectrics placed against the vertical toroid walls and extend to the waveguide walls is quite effective. A useful configuration is a combination of the temperature-compensated garnets (gadolinium doped YIG) fabricated into thin-walled toroids used with dielectric elements having high thermal conductivities.

Figure 5 shows the variation of differential phase shift with average power in a sample of 15% Gd, 0.5% Dy, 15.5% Al doped YIG. The measurements were made at S-band. Two geometrically different conducting elements were used and are referred to as configuration A (boron slabs adjacent to the vertical ferrite walls to conduct heat to the broad waveguide walls) and configuration B ("T"-shaped boron nitride elements oriented so that the bar of the "T" contacts and thus conducts heat to the narrow walls of the waveguide). The length of this bar is equal to the waveguide height. The most significant dimension of the "T"-shaped elements is the thickness (X) of the leg of the "T". Figure 5 shows that the greatest stability (only an 8.6% decrease (PD) of phase shift) with average power up to 700 watts occurred when $X = \frac{1}{2}W_5$. The 15 percent gadolinium doped YIG has been found to lead to maximum stability of phase shift with average power. Further increases in doping level increase the loss to such an extent that overall stability is reduced.

Table I indicates some of the trade offs necessary to achieve high peak and average power levels. Some of these results represent data already achieved; some are predicted performance levels based on the computer-aided solution, together with experimental results.

1. J.L. Allen, "The Analysis of Ferrite Phase Shifters Including the Effects of Losses", Ph.D. Dissertation, Georgia Institute of Technology, May 1966.
2. B. Lax, K.J. Button, and L.M. Roth, "Ferrite Phase Shifters in Rectangular Waveguide", Journal of Applied Physics, Vol. 25, p. 1413, 1954.
3. W.J. Ince and E. Stern, "Non-Reciprocal Phase Shifters in Rectangular Waveguide", IEEE International Convention Record, Part 5, p. 33, 1966.
4. T-shaped boron nitride thermal elements suggested by D. Temme and E. Stern of MIT Lincoln Laboratory.

TABLE I. FERRITE DIGITAL PHASE SHIFTER PHASE SHIFT, LOSS AND POWER TRADE-OFFS **

Band	Pp(Kw)	Pav(W)	$4\pi M_s$	$\Delta\phi$/inch	LP 360°	Notes
X*	1	1	1800	150	0.35	(1)
X*	150	1	900	60	0.70	(1)
X*	100	350	1000	60	1.00	(2)(B)
C	1	1	1800	160	0.40	(1)
C	300	1	500	40	0.70	(1)
C	300	700	650	30	1.00	(2)(B)
C*	50	500	825	38	0.65	(2)(A)
S	1	1	770	57	0.50	(1)
S	500	1	335	23	0.95	(1)
S	500	1000	350	20	1.00	(2)(B)
S*	175	800	425	26	0.95	(2)(B)

* Actual Measured Results

** { $\Delta\phi$/inch values shown are for low power, room temperature
LP 360° values shown are for operational devices at indicated power levels }

(A) Water cooled with Boron Nitride Cooling Slabs

(B) Water cooled with Boron Nitride Thermal Conducting "T" Sections

(1) Al Doped YIG

(2) Gd, Al Doped YIG

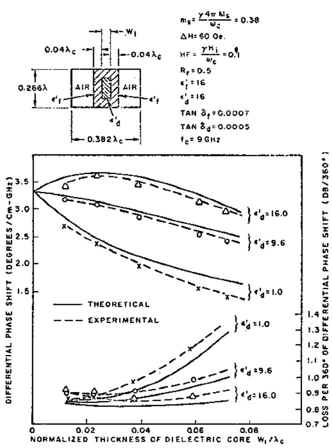

FIG. 1 - Differential Phase Shift and Loss per 360 Differential Phase Shift for Several Dielectric Loads

DATA POINT	COMPOSITION	$\gamma 4\pi M_s/\omega_c$	R_R	ΔH_{poly} (oe)	ΔH_{int} (oe)
1	10% DY SUBSTITUTED YIG	0.30	0.60	380	~365
2	4% DY " "	0.35	0.57	160	~145
3	2% DY " "	0.35	0.65	100	~85
4	30% GD " "	0.39	0.55	70	~50
5	15% GD " "	0.48	0.63	50	~25
6	YIG	0.43	0.57	30	~12
7	MG MN FERRITE	0.64	0.67	510	~18

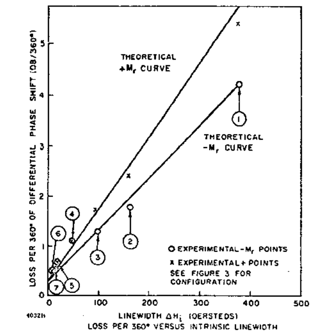

FIG. 2 - Loss per 360° Versus Intrinsic Linewidth

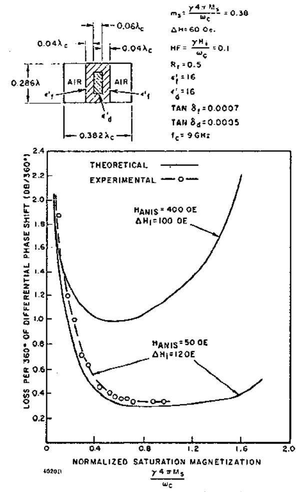

FIG. 3 - Variation of Loss per 360° of Differential Phase Shift with Normalized Saturation Magnitization

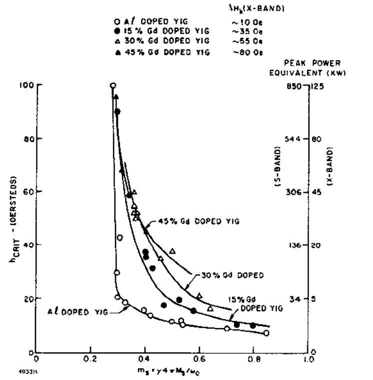

FIG. 4 - Ferrite Critical Field Dependence on Magnetization

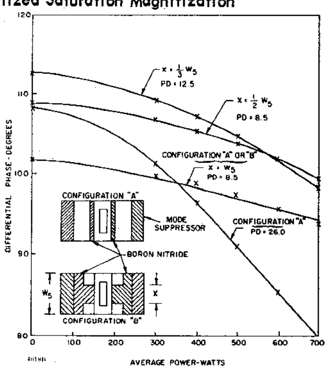

FIG. 5 - Differential Phase vs Average Power for Various Phase Shifter Configurations